ICAS-88-3.3.2

OPTIMIZATION AND GUIDANCE OF LANDING TRAJECTORIES IN A WINDSHEAR[1,2]

A. Miele[3], T. Wang[4], and W. W. Melvin[5]
Rice University, Houston, Texas
Delta Airlines, Atlanta, Georgia

Abstract. This paper is concerned with the optimization and guidance of landing trajectories in the presence of windshear. Two aspects of the problem are considered, abort landing and penetration landing. In the former,the only control is the angle of attack, since maximum power setting is employed; in the latter, two controls are involved, the angle of attack and the power setting.

For abort landing, optimal trajectories are determined by minimizing the peak value of the altitude drop. In relatively severe windshears, the optimal trajectory includes three branches: a descending flight branch, followed by a nearly horizontal flight branch, followed by an ascending flight branch, after the aircraft has passed through the shear region. The maximum altitude drop increases with the windshear intensity and the initial altitude. The point of minimum velocity occurs at the end of the shear.

For penetration landing, optimal trajectories are determined by minimizing a performance index measuring the deviation of the altitude of the flight trajectory from that of the nominal trajectory, subject to three requirements: the touchdown path inclination is specified; the touchdown velocity tolerance is specified; and the touchdown distance tolerance is specified. In a relatively severe windshear, the optimal trajectory deviates somewhat from the nominal trajectory in the shear region, but recovers the nominal trajectory in the aftershear region. The deviation increases with the windshear intensity and the initial altitude. The point of minimum velocity occurs at the end of the shear.

Next, guidance trajectories are developed for both abort landing and penetration landing. The main idea is to preserve the properties of the optimal trajectories, while employing only local information on the windshear intensity and the downdraft.

The abort landing guidance scheme is akin to the guidance scheme already developed for take-off trajectories. The angle of attack is determined by the relative acceleration, the windshear intensity, and the downdraft.

The penetration landing guidance scheme is constructed in such a way that the angle of attack

[1]Paper presented at the 16th Congress of the International Council of the Aeronautical Sciences, Jerusalem, Israel, August 28-September 2, 1988 (Paper No. ICAS-88-332).

[2]This research was supported by NASA Langley Research Center, Grant No. NAG-1-516, by Boeing Commercial Airplane Company (BCAC), and by Air Line Pilots Association (ALPA). The authors are indebted to Dr. R.L. Bowles (NASA-LRC) and Dr. G. R. Hennig (BCAC) for helpful discussions.

[3]Professor of Aerospace Sciences and Mathematical Sciences, Aero-Astronautics Group, Rice University, Houston, Texas. Fellow AIAA.

[4]Senior Research Scientist, Aero-Astronautics Group, Rice University, Houston, Texas. Member AIAA.

[5]Captain, Delta Airlines, Atlanta, Georgia; and Chairman, Airworthiness and Performance Committee, Air Line Pilots Association (ALPA), Washington, DC. Member AIAA.

is determined by the windshear intensity, the absolute path inclination, and the glide slope angle, while the power setting is determined by the windshear intensity and the relative velocity. For the particular case of a low-altitude windshear encounter, the penetration landing guidance scheme is simplified further by controlling the angle of attack via absolute path inclination signals, while keeping the power setting at the maximum permissible value.

Key Words. Flight mechanics, take-off, abort landing, penetration landing, optimal trajectories, sequential gradient-restoration algorithm, guidance, feedback control.

Nomenclature

D = drag force, lb;

g = acceleration of gravity, ft sec^{-2};

h = altitude, ft;

L = lift force, lb;

m = mass, lb ft^{-1} sec^2;

T = thrust force, lb;

V = relative velocity, ft sec^{-1};

W = mg = weight, lb;

W_h = h-component of wind velocity, ft sec^{-1};

W_x = x-component of wind velocity, ft sec^{-1};

x = horizontal distance, ft;

α = relative angle of attack (wing), rad;

β = engine power setting;

γ = relative path inclination, rad;

γ_e = absolute path inclination, rad;

γ_g = glide slope angle, rad;

δ = thrust inclination, rad;

θ = pitch attitude angle (wing), rad;

λ = wind intensity parameter;

τ = final time, sec;

GT = guidance trajectory;

NT = nominal trajectory;

OT = optimal trajectory;

SGT= simplified guidance trajectory.

1. Introduction

Low-altitude windshear is a threat to the safety of aircraft in take-off and landing (Ref. 1). Over the past 20 years, some 30 aircraft accidents have been attributed to windshear. The most notorious ones are the crash of PANAM Flight 759 on July 9, 1982 at New Orleans International Airport (Boeing B-727 in take-off, Ref. 2) and the crash of Delta Airlines Flight 191 on August 2, 1985 at Dallas-Fort Worth International Airport (Lockheed L-1011 in landing, Refs. 3-5).

Low-altitude windshear is usually associated with a severe meteorological phenomenon, called the downburst. In turn, a downburst involves a descending column of air, which then spreads horizontally in the neighborhood of the ground. This condition is hazardous, because an aircraft in take-off or landing might encounter a headwind coupled with a downdraft, followed by a tailwind coupled with a downdraft. The transition from headwind to tailwind engenders a transport acceleration, and hence a windshear inertia force (the product of the transport acceleration and the mass of the aircraft). In turn, the windshear inertia force can be as large as the drag of the aircraft, and in some cases as large as the thrust of engines. Hence, an inadvertent encounter with a low-altitude windshear can be a serious problem for even a skilled pilot.

This paper is concerned with the landing problem. When the pilot of an aircraft on a glide path detects an inadvertent encounter with a low-altitude windshear, he must choose between abort

landing (see Refs. 6-10) and penetration landing (see Refs. 11-14). Clearly, if the initial altitude is high enough, abort landing is a safer procedure than penetration landing; on the other hand, if the initial altitude is low enough, the opposite might be true: in low-altitude penetration landing, the aircraft might have to traverse only a part of shear region; in low-altitude abort landing, the aircraft might have to traverse the whole of the shear region.

In this paper, which is based on Refs. 8-12, we discuss both the abort landing and the penetration landing. In the former, the only control is the angle of attack, since maximum power setting is employed; in the latter, two controls are involved, the angle of attack and the power setting.

1.1. Abort Landing. Optimal trajectories are determined by minimizing the peak value of the altitude drop. The resulting optimization problem is a minimax problem or Chebyshev problem of optimal control, which can be converted into a Bolza problem via suitable transformations. Then, numerical solutions are obtained with the sequential gradient-restoration algorithm (Refs. 15-16).

Next, guidance trajectories are considered, based on the idea of preserving the properties of the optimal trajectories, while employing only local information on the state of the aircraft and the wind. The guidance scheme presented here is an acceleration guidance scheme, akin to that already developed for take-off trajectories (Ref. 17). The angle of attack is determined by the relative acceleration, the windshear intensity, and the downdraft. For alternative guidance schemes (target altitude guidance, safe target altitude guidance, gamma guidance, and modified constant pitch guidance), see Refs. 9-10.

1.2. Penetration Landing. Optimal trajectories are determined by minimizing a performance index measuring the deviation of the altitude of the flight trajectory from that of the nominal trajectory, subject to three requirements: the touchdown path inclination is specified (-0.5 deg); the touchdown velocity tolerance is specified ($\pm$ 30 knots); and the touchdown distance tolerance is specified ($\pm$ 1000 ft). The resulting optimization problem is a Bolza problem of optimal control, which is solved numerically with the sequential gradient-restoration algorithm (Refs. 15-16).

Next, guidance trajectories are considered. The guidance scheme presented here is such that the angle of attack is determined by the windshear intensity, the absolute path inclination, and the glide slope angle, while the power setting is determined by the windshear intensity and the relative velocity. For the particular case of a low-altitude windshear encounter, the penetration landing guidance scheme is simplified further by controlling the angle of attack via absolute path inclination signals, while keeping the power setting at the maximum permissible value.

2. System Description

In this paper, we make use of the relative wind-axes system in connection with the following assumptions: (a) the aircraft is a particle of constant mass; (b) flight takes place in a vertical plane; (c) Newton's law is valid in an Earth-fixed system; and (d) the wind flow field is steady.

With above premises, the equations of motion include the kinematical equations

$$\dot{x} = V\cos\gamma + W_x, \tag{1a}$$

$$\dot{h} = V\sin\gamma + W_h, \tag{1b}$$

and the dynamical equations

$$\dot{V} = (T/m)\cos(\alpha + \delta) - D/m - g\sin\gamma - (\dot{W}_x\cos\gamma + \dot{W}_h\sin\gamma), \tag{2a}$$

$$\dot{\gamma} = (T/mV)\sin(\alpha + \delta) + L/mV - (g/V)\cos\gamma + (1/V)(\dot{W}_x\sin\gamma - \dot{W}_h\cos\gamma). \tag{2b}$$

Because of assumption (d), the total derivatives of the wind velocity components and the corresponding partial derivatives satisfy the relations

$$\dot{W}_x = (\partial W_x/\partial x)(V\cos\gamma + W_x) + (\partial W_x/\partial h)(V\sin\gamma + W_h), \tag{3a}$$

$$\dot{W}_h = (\partial W_h/\partial x)(V\cos\gamma + W_x) + (\partial W_h/\partial h)(V\sin\gamma + W_h). \tag{3b}$$

These relations must be supplemented by the functional relations

$$T = T(h,V,\beta), \tag{4a}$$

$$D = D(h,V,\alpha), \qquad L = L(h,V,\alpha), \tag{4b}$$

$$W_x = W_x(x,h), \qquad W_h = W_h(x,h), \tag{4c}$$

and by the analytical relations

$$\gamma_e = \arctan[(V\sin\gamma + W_h)/(V\cos\gamma + W_x)], \tag{5a}$$

$$\theta = \alpha + \gamma. \tag{5b}$$

For a given value of the thrust inclination δ, the differential system (1)-(4) involves four state variables [the horizontal distance $x(t)$, the altitude $h(t)$, the velocity $V(t)$, and the relative path inclination $\gamma(t)$] and two control variables [the angle of attack $\alpha(t)$ and the power setting $\beta(t)$]. However, the number of control variables reduces to one (the angle of attack), if the power setting is specified in advance. The quantities defined by the analytical relations (5) can be computed a posteriori, once the values of the state and the control are known.

2.1. Inequality Constraints. The angle of attack α and its time derivative $\dot{\alpha}$ are subject to the inequalities

$$\alpha \leq \alpha_*, \tag{6a}$$

$$-\dot{\alpha}_* \leq \dot{\alpha} \leq \dot{\alpha}_*, \tag{6b}$$

where α_* is a prescribed upper bound and $\dot{\alpha}_*$ is a prescribed, positive constant.

The power setting β and its time derivative $\dot{\beta}$ are subject to the inequalities

$$\beta_* \leq \beta \leq 1, \tag{7a}$$

$$-\dot{\beta}_* \leq \dot{\beta} \leq \dot{\beta}_*, \tag{7b}$$

where β_* is a prescribed lower bound and $\dot{\beta}_*$ is a prescribed, positive constant.

For the optimal trajectories, Ineqs. (6) and (7) are enforced indirectly via transformation techniques converting the inequality constraints into equality constraints (see Refs. 8,11 for details).

2.2. Aircraft. All of the numerical data presented in this paper refer to the Boeing B-727 aircraft powered by three JT8D-17 turbofan engines. It is assumed that: the runway is located at sea level altitude; the ambient tmeperature is 100 deg F; the gear is down; the flap setting is $\delta_F = 30$ deg; the landing weight is W = 150,000 lb.

The inequality constraints (6) on the angle

of attack are enforced with

$$\alpha_* = 17.2 \text{ deg}, \tag{8a}$$

$$\dot{\alpha}_* = 3.0 \text{ deg sec}^{-1}. \tag{8b}$$

The inequality constraints (7) on the power setting are enforced with

$$\beta_* = 0.25, \tag{9a}$$

$$\dot{\beta}_* = 0.30 \text{ sec}^{-1}, \tag{9b}$$

2.3. Wind Model. In this paper, the following particular form of Eqs. (4c) is assumed:

$$W_x = \lambda A(x), \tag{10a}$$

$$W_h = \lambda (h/h_*) B(x), \tag{10b}$$

with

$$\lambda = \Delta W_x / \Delta W_{x_*}. \tag{10c}$$

The function A(x) represents the distribution of the horizontal wind versus the horizontal distance (Fig. 1); the function B(x) represents the distribution of the vertical wind versus the horizontal distance (Fig. 1); the parameter λ characterizes the intensity of the shear/downdraft combination; ΔW_x is the horizontal wind velocity difference (maximum tailwind minus maximum headwind); $\Delta W_{x_*} = 100$ ft sec^{-1} is a reference value for the horizontal wind velocity difference; and $h_* = 1000$ ft is a reference value for the altitude.

The one-parameter family of wind models (10) has the following properties: (a) it represents the transition from a uniform headwind to a uniform tailwind, with nearly constant shear in the core of the downburst; (b) the downdraft achieves maximum negative value at the center of the downburst; (c) the downdraft vanishes at h = 0; and (d) the functions W_x, W_h nearly satisfy the continuity equation and the irrotationality condition in the core of the downburst. For previous literature on wind models, see Ref. 18.

Decreasing values of λ (hence, decreasing values of ΔW_x) correspond to milder windshears; conversely, increasing values of λ (hence, increasing values of ΔW_x) correspond to more severe windshears. If one excludes the 1983 windshear episode at Andrews AFB, the highest value of λ ever recorded is $\lambda = 1.40$, corresponding to $\Delta W_x = 140$ ft sec^{-1}. Hence, in this paper, the following values of λ and ΔW_x are considered:

$$\lambda = 1.00,\ 1.20,\ 1.40, \tag{11a}$$

$$\Delta W_x = 100,\ 120,\ 140 \text{ ft sec}^{-1}. \tag{11b}$$

3. Abort Landing Problem

In this section, we discuss two aspects of the abort landing problem: optimization and guidance. Also, we present numerical results comparing the optimal trajectories (OT) and the guidance trajectories (GT).

3.1. Optimization. In determining optimal abort landing trajectories, we employ the following assumptions: (i) maximum power setting is employed; namely,the power setting β is increased from the initial value β_0 to the maximum value $\beta = 1$ at a constant time rate $\dot{\beta}_0 = 0.2$ sec^{-1}; afterward, the maximum value $\beta = 1$ is maintained; hence, the only control is the angle of attack; (ii) the constraints (1)-(7) must be satisfied; (iii) the initial conditions are given; and (iv) at the final point, gamma recovery is required, that is,

$$\gamma_\tau = \gamma_*, \tag{12}$$

where γ_* is the path inclination for quasi-steady steepest climb (Ref. 8).

The performance index being minimized is the peak value of the modulus of the difference between the instantaneous altitude h and a reference value h_R,

$$I = \max_t |h_R - h|, \qquad 0 \leq t \leq \tau; \quad (13)$$

here, $h_R = h_* = 1000$ ft is a constant.

This is a minimax problem or Chebyshev problem of optimal control. It can be reformulated as a Bolza problem of optimal control, in which one minimizes the integral performance index

$$J = \int_0^\tau (h_R - h)^q dt, \qquad (14)$$

for large values of the positive, even exponent q.

Data. The computations presented here refer to the Boeing B-727 aircraft of Section 2.2 and the wind model of Section 2.3. The following conditions are assumed at the initial point:

$$x_0 = 0 \text{ ft}, \qquad (15a)$$

$$h_0 = 200, 600, 1000 \text{ ft}, \qquad (15b)$$

$$V_0 = 239.7 \text{ ft sec}^{-1}, \qquad (15c)$$

$$\gamma_{e0} = -3.0 \text{ deg}, \qquad (15d)$$

and at the final point:

$$\gamma_\tau = 7.431 \text{ deg}; \qquad (16a)$$

the final time is assumed to be

$$\tau = 40 \text{ sec}. \qquad (16b)$$

For the windshear model assumed, this time is about twice the duration of the windshear encounter ($\Delta t = 22$ sec).

Results. Numerical results were obtained using the sequential gradient-restoration algorithm in conjunction with the primal formulation (Refs. 15-16). These results are shown in Figs. 2-3 for different combinations of initial altitude h_0 and wind velocity difference ΔW_x. Specifically, Fig. 2 shows the effect of the initial altitude on the optimal trajectory for a given value of the wind velocity difference ($\Delta W_x = 120$ ft sec^{-1}); and Fig. 3 shows the effect of the wind velocity difference on the optimal trajectory for a given value of the initial altitude ($h_0 = 600$ ft). Each figure contains two parts: the altitude h versus the time t; and the velocity V versus the time t. From Figs. 2-3, the following comments arise:

(a) the optimal trajectory includes three branches: a descending flight branch, followed by a nearly horizontal flight branch, followed by an ascending flight branch after the aircraft has passed through the shear region; the maximum altitude drop depends on the windshear intensity and the initial altitude, increasing as the windshear intensity and the initial altitude increase;

(b) the velocity decreases in the shear region and increases in the aftershear region; the point of minimum velocity occurs at the end of the shear; the value of the minimum velocity is nearly independent of the windshear intensity and the initial altitude;

(c) the angle of attack (not shown in Figs. 2-3) exhibits an initial dip, followed by a gradual, sustained increase; the maximum value of the angle of attack is reached at about the end of the shear; then, the angle of attack decreases

gradually in the aftershear region (see Ref. 8).

3.2. Guidance. Here, we present an acceleration guidance scheme, based on the relative acceleration, whose objective is to approximate the behavior of the optimal trajectory in a windshear. While the optimal trajectory is based on global information on the wind distribution, the guidance scheme relies on local information on the windshear and the downdraft.

The acceleration guidance scheme is a modification of the guidance scheme bearing the same name, already developed for take-off trajectories (Ref. 17). The modification accounts for these facts and ideas:

(i) in abort landing, the initial path inclination is descending; in take-off, it is ascending;

(ii) an abort landing trajectory can be viewed as a transition from a descending trajectory to an ascending trajectory;

(iii) if the abort landing maneuver is initiated at high altitude, containing the velocity loss should have priority over containing the altitude drop;

(iv) if the abort landing maneuver is initiated at low altitude, containing the altitude drop should have priority over containing the velocity loss.

Guidance Law. The guidance law includes three parts, one pertaining to the descending flight branch, one pertaining to the nearly horizontal flight branch, and one pertaining to the ascending flight branch:

(a) for the descending flight branch, the key property is that the velocity decrease is relatively low; hence, the descent guidance law is governed by the rule $\dot{V}/g = 0$;

(b) for the nearly-horizontal flight branch, the key property is that the instantaneous deceleration is approximately proportional to the shear-downdraft factor F, introduced in Ref. 17; hence, the recovery guidance law is governed by the rule $\dot{V}/g + C_1 F = 0$, where $C_1 = 0.5$;

(c) for the ascending flight branch, the key property is that the instantaneous path inclination tends to a positive value; consistently, the velocity tends toward a value somewhat smaller than the initial value V_0; hence, the ascent guidance law is governed by the rule $V/V_0 - C_2 = 0$, where $C_2 = 5/6$.

Feedback Control. The above guidance law can be implemented in the feedback control form given below:

$$\alpha - \tilde{\alpha}(V) = K_1(\dot{V}/g + C_1 F) + K_2(V/V_0 - C_2), \qquad (17a)$$

$$F = (\dot{W}_x/g)\cos\gamma + (\dot{W}_h/g)\sin\gamma - W_h/V$$

$$\cong \dot{W}_x/g - W_h/V, \qquad (17b)$$

$$\alpha \leq \alpha_*, \quad -\dot{\alpha}_* \leq \dot{\alpha} \leq \dot{\alpha}_*. \qquad (17c)$$

Here, $\tilde{\alpha}(V)$ is the nominal angle of attack (Ref. 17); F is the shear-downdraft factor; K_1, K_2 are the gain coefficients; and C_1, C_2 are constants. The values of the gain coefficients and the constants are given in Table 1.

Note that, for the descent guidance and the recovery guidance, the velocity control is bypassed ($K_2 = 0$). Also note that, for the ascent guidance, $F = 0$; hence, the feedback control becomes a velocity control.

Table 1. Gain coefficients and constants.

Guidance	K_1 (rad)	C_1	K_2(rad)	C_2
Descent	10	0.0	0.00	0.00
Recovery	10	0.5	0.00	0.00
Ascent	10	0.0	0.72	0.83

Switch Criteria. In the acceleration guidance scheme, one must define (i) a switch criterion governing the transition from descent guidance to recovery guidance and (ii) a switch criterion governing the transition from recovery guidance to ascent guidance.

(i) The transition from descent guidance to recovery guidance must be performed when a certain target altitude has been reached. The target altitude is somewhat above the minimum altitude of the optimal trajectory and is given by (Ref. 10)

$$h_T = 0.76h_0 + (0.336 - 1.70\dot{W}_x/g)h_*, \tag{18a}$$

$$0.2h_* \leq h_T \leq 0.9h_0, \tag{18b}$$

where $\dot{W}_x$ is the instantaneous horizontal wind acceleration. The lower bound in (18) prevents ground contact due to excessive undershooting of the target altitude; the upper bound in (18) prevents early transition from descent guidance to recovery guidance.

(ii) The transition from recovery guidance to ascent guidance must be performed when the shear region is past and the velocity starts to increase; that is, it must be performed when the instantaneous acceleration $\dot{V}$ switches from negative to positive. An added condition is that the rate of climb be higher than a threshold value, for example, $\dot{h} \geq 0.05\ V_0$.

(iii) There is also a bypass criterion, namely: the descent guidance is bypassed if $h_0 \leq 0.2\ h_*$, where $h_* = 1000$ ft.

Results. Numerical results were obtained for the acceleration guidance scheme, which was implemented in the feedback control form (17), with gain coefficients and constants supplied by Table 1. These results are shown in Figs. 2-3 for different combinations of initial altitude h_0 and wind velocity difference ΔW_x. From the numerical solutions, upon comparing the guidance trajectories (GT) and the optimal trajectories (OT), certain general conclusions become apparent:

(a) both the GT and the OT include a descending flight branch, followed by a nearly horizontal flight branch, followed by an ascending flight branch, after the aircraft has passed through the shear region;

(b) for both the GT and the OT, the peak altitude drop depends on the initial altitude and the windshear intensity, increasing as the initial altitude and the windshear intensity increase; as expected, the minimum altitude of the GT is slightly lower than the minimum altitude of the OT;

(c) for both the GT and the OT, the point of minimum velocity is achieved near the end of the shear; in the range of initial altitudes and windshear intensities considered, the minimum velocity of the GT is nearly independent of h_0 and ΔW_x;

(d) the minimum velocity of the GT is slightly larger than the minimum velocity of the OT; the higher minimum velocity of the GT (with respect to the OT) is consistent with the lower minimum altitude of the GT (with respect to the OT);

(e) for both the GT and the OT, the angle of attack exhibits an initial decrease, followed by a gradual, sustained increase; the peak value of the angle of attack is achieved near the end of the shear; the function $\alpha(t)$ of the OT is smoother than the function $\alpha(t)$ of the GT (see Ref. 10); for the GT, relatively large oscillations of the angle of attack occur near the point of switch from descent guidance to recovery guidance; these oscillations can be reduced by employing some more sophisticated form of feedback control than the simple proportional feedback control considered here.

4. Penetration Landing Problem

In this section, we discuss two aspects of the penetration landing problem: optimization and guidance. Also, we present numerical results comparing the optimal trajectories (OT), the guidance trajectories (GT), and the simplified guidance trajectories (SGT).

4.1. Optimization. In determining optimal penetration landing trajectories, we employ the following assumptions: (i) variable power setting is employed; hence, both the angle of attack and the power setting are regarded as controls; (ii) the constraints (1)-(7) must be satisifed; (iii) the initial conditions are given; (iv) at the final point, the airplane must land with a specified path inclination and within specified tolerances for the velocity and the distance, that is,

$$\gamma_{e\tau} - \tilde{\gamma}_{e\tau} = 0, \tag{19a}$$

$$|V_\tau - \tilde{V}_\tau| \leq A, \tag{19b}$$

$$|x_\tau - \tilde{x}_\tau| \leq B; \tag{19c}$$

here, the tilde denotes the nominal conditions and A, B denote the specified tolerances for the velocity and the distance. Ineqs. (19b) and (19c) are enforced indirectly via transformation techniques converting the inequality constraints into equality constraints (see Refs. 11-12 for details).

The performance index being minimized measures the deviation of the altitude of the flight trajectory from that of the nominal trajectory, that is,

$$I = \int_0^\tau [h - \tilde{h}(x)]^2 dt. \tag{20}$$

In turn, the nominal altitude distribution $\tilde{h}(x)$ involves two parts: the approach part, in which the absolute path inclination is constant ($\gamma_e = \gamma_{e0} = -3.0$ deg); and the flare part, in which the absolute path inclination varies linearly between the approach value and the touchdown value ($\gamma_{e\tau} = -0.5$ deg).

Data. The computations presented here refer to the Boeing B-727 aircraft of Section 2.2 and the wind model of Section 2.3. The following conditions are assumed at the initial point ($t = 0$):

$$x_0 = 0 \text{ ft}, \tag{21a}$$

$$h_0 = 200, 600, 1000 \text{ ft}, \tag{21b}$$

$$V_0 = 239.7 \text{ ft sec}^{-1}, \tag{21c}$$

$$\gamma_{e0} = -3.0 \text{ deg}, \tag{21d}$$

and at the final point ($h_\tau = 0$):

$$\gamma_{e\tau} = -0.5 \text{ deg}, \tag{22a}$$

$$|V_\tau - \tilde{V}_\tau| \leq 30 \text{ knots} = 50.6 \text{ ft sec}^{-1}, \tag{22b}$$

$$|x_\tau - \tilde{x}_\tau| \leq 1000 \text{ ft}, \tag{22c}$$

with

$$\tilde{V}_\tau = V_0 = 239.7 \text{ ft sec}^{-1}, \tag{23}$$

and

$$\tilde{x}_\tau = 4498 \text{ ft}, \quad \text{if } h_0 = 200 \text{ ft}, \tag{24a}$$

$$\tilde{x}_\tau = 12130 \text{ ft}, \quad \text{if } h_0 = 600 \text{ ft}, \tag{24b}$$

$$\tilde{x}_\tau = 19763 \text{ ft}, \quad \text{if } h_0 = 1000 \text{ ft}. \tag{24c}$$

The final time τ is free and is to be determined.

Results. Numerical results were obtained using the sequential gradient-restoration algorithm in conjunction with the primal formulation (Refs. 15-16). These results are shown in Figs. 4-5 for several combinations of initial altitude h_0 and wind velocity difference ΔW_x. Specifically, Fig. 4 shows that the effect of the wind velocity difference on the optimal trajectory for h_0 = 600 ft, and Fig. 5 shows the effect of the wind velocity difference on the optimal trajectory for h_0 = 200 ft. Each figure contains two parts: the altitude h versus the distance x; and the velocity V versus the distance x. From Figs. 4-5, the following comments arise:

(a) depending on the windshear intensity, the optimal trajectory (OT) deviates somewhat from the nominal trajectory (NT) in the shear region; however, the optimal trajectory recovers the nominal trajectory in the aftershear region;

(b) the velocity decreases in the shear region and increases in the aftershear region; the point of minimum velocity occurs at the end of the shear; the value of the minimum velocity is nearly independent of the windshear intensity;

(c) the angle of attack (not shown in Figs. 4-5) exhibits an initial dip, followed by a gradual, sustained increase; the maximum value of the angle of attack is reached at about the end of the shear; then, the angle of attack decreases gradually in the aftershear region (see Ref. 11);

(d) the power setting (not shown in Figs. 4-5) increases quickly to the maximum value; the maximum value is maintained in the shear region; then, the power setting decreases gradually in the aftershear region (see Ref. 11);

(e) the optimal trajectory meets the touchdown requirements (22) in the range of initial altitudes [see (21b)] and windshear intensities [see (11)] considered.

4.2. Guidance. Here, we present a penetration landing guidance scheme, whose objective is to approximate the behavior of the optimal trajectory in a windshear. While the optimal trajectory is based on global information on the wind distribution, the guidance scheme relies on local information on the windshear and the downdraft.

The penetration landing guidance scheme accounts for these facts and ideas:

(i) there are three touchdown requirements to be met, those concerning the path inclination, the velocity, and the distance; there is also one additional requirement, namely, the deviation of the flight trajectory from the nominal trajectory is to be small;

(ii) while the total number of requirements is four, there are only two controls available, namely, the power setting and the angle of attack; however, for the purposes of constructing a guidance scheme, the coupling relation between the power setting and the angle of attack can be ignored; see the separation result established in Ref. 12;

(iii) the power setting is employed to meet the touchdown velocity requirement;

(iv) the angle of attack is employed to meet the three remaining requirements; since satisfying

the small deviation requirement implies satisfying the distance requirement, it is sufficient to employ the angle of attack to meet only two requirements, namely, the path inclination requirement and the small deviation requirement (glide slope requirement);

(v) for guidance purposes, the path inclination requirement can be relaxed from the equality $\gamma_{e\tau} - \tilde{\gamma}_{e\tau} = 0$ to the inequality $|\gamma_{e\tau} - \tilde{\gamma}_{e\tau}| \leq C$, where $C = 0.5$ deg.

Guidance Laws. The guidance laws are two, one concerning the power setting and one concerning the angle of attack:

(a) for the power setting, the key property is that maximum power setting is employed in the shear region and velocity recovery is achieved in the aftershear region; hence, the power setting guidance law is governed by the rule $\beta = 1$ in the shear region and the rule $V = V_0$ in the aftershear region;

(b) for the angle of attack, the guidance law is more complex, since the requirements are more complex; if there is no windshear or if the windshear is weak, the absolute path inclination γ_e is constant along the approach path ($h \geq h_f$) and is linear with the altitude along the flare path ($h \leq h_f$); under the same conditions, the glide slope γ_g is constant along the approach path ($h \geq h_f$), while it is not defined along the flare path ($h \leq h_f$); on the other hand, if there is windshear and if the windshear is strong-to-severe, both the absolute path inclination and the glide slope must be corrected for windshear effects, which increase as the shear/downdraft factor and the altitude increase; hence, the angle of attack guidance law is governed by rules of the form $\gamma_e = \tilde{\gamma}_e(h,F)$, $\gamma_g = \tilde{\gamma}_g(h,F)$, where h is the altitude and F is the shear/downdraft factor [see (17b)].

Feedback Control. For the power setting, the guidance law can be implemented in the following feedback control form:

$$\beta - \beta_0 = -K_1(V/V_0 - 1) + K_2F, \tag{25a}$$

$$F = \dot{W}_x/g - W_h/V, \tag{25b}$$

$$K_1 = (1 - \beta_0)V_0/A, \tag{25c}$$

$$K_2 = (1 - \beta_0)/F_c, \tag{25d}$$

$$\beta_* \leq \beta \leq 1, \quad -\dot{\beta}_* \leq \dot{\beta} \leq \dot{\beta}_*. \tag{25e}$$

Here, β is the instantaneous power setting and $\beta_0 = 0.3330$ is the nominal power setting in the absence of windshear; V is the instantaneous velocity, $V_0 = 239.7$ ft sec^{-1} is the nominal velocity, and $A = 50.6$ ft sec^{-1} is the touchdown velocity tolerance; F is the shear/downdraft factor and $F_c = 1/8 = 0.1250$ is a threshold value for the shear/downdraft factor; $K_1 = 3.15$ is the gain coefficient for velocity error and $K_2 = 5.34$ is the shear/downdraft gain coefficient.

The power setting feedback control law (25) employs both velocity signals and shear/downdraft signals. In the shear region, $F \neq 0$; the power setting response is such that, as F increases, the value of β increases, tending quickly to the maximum value $\beta = 1$ as F reaches the threshold value F_c. In the aftershear region, $F = 0$; hence, the feedback control becomes a velocity control.

For the angle of attack, the guidance law can be implemented in the following feedback control form:

$$\alpha - \tilde{\alpha}(V) = -K_3[\gamma_e - \tilde{\gamma}_e(h,F)] - K_4[\gamma_g - \tilde{\gamma}_g(h,F)], \quad (26a)$$

$$F = \dot{W}_x/g - W_h/V, \quad (26b)$$

$$K_3 = 5, \quad K_4 = 5(h/h_f - 1), \quad h \geq h_f, \quad (26c)$$

$$K_3 = 5, \quad K_4 = 0, \quad h \leq h_f, \quad (26d)$$

$$\alpha \leq \alpha_*, \quad -\dot{\alpha}_* \leq \dot{\alpha} \leq \dot{\alpha}_*. \quad (26e)$$

Here, α is the instantaneous angle of attack and $\tilde{\alpha}(V)$ is the nominal angle of attack (Ref. 17); γ_e is the instantaneous absolute path inclination and $\tilde{\gamma}_e(h,F)$ is the nominal absolute path inclination; γ_g is the instantaneous glide slope and $\tilde{\gamma}_g(h,F)$ is the nominal glide slope; h is the instantaneous altitude and h_f = 50 ft is the altitude at the end of the approach path/beginning of the flare path; K_3 is the gain coefficient for absolute path inclination error and K_4 is the gain coefficient for glide slope error. In turn, the nominal absolute path inclination and the nominal glide slope are given by

$$\tilde{\gamma}_e = \gamma_{e0} - \psi, \quad h \geq h_f, \quad (26f)$$

$$\tilde{\gamma}_e = \gamma_{e0}h/h_f + \gamma_{e\tau}(1 - h/h_f), \quad h \leq h_f, \quad (26g)$$

$$\tilde{\gamma}_g = \gamma_{e0} + \psi, \quad h \geq h_f, \quad (26h)$$

$$\tilde{\gamma}_g = \text{undefined}, \quad h \leq h_f, \quad (26i)$$

with γ_{e0} = -3.0 deg, $\gamma_{e\tau}$ = -0.5 deg. The symbol ψ denotes the correction to the absolute path inclination and the glide slope due to windshear effects. This correction is given by

$$\psi = 0.002\ (1 - F_c/F)(h/h_f - 1), \quad (26j)$$

$$h \geq h_f, \quad F \geq F_c; \quad (26k)$$

it vanishes for weak-to-moderate windshears and/or lower altitudes, but becomes increasingly larger for strong-to-severe windshears and higher altitudes.

The angle of attack feedback control law (26) employs absolute path inclination signals, glide slope signals, and windshear signals. The function of the absolute path inclination signals is to make sure that the touchdown absolute path inclination requirement is met. The function of the glide slope signals is to make sure that the guidance trajectory is geometrically close to the nominal trajectory. The function of the windshear signals is to contain the velocity loss due to windshear action by allowing more altitude loss at higher altitudes; hence, at lower altitudes, sufficient velocity is available so that the aircraft can be controlled effectively.

The gain coefficients in (26) are such that their ratio is given by

$$K_4/K_3 = h/h_f - 1, \quad h \geq h_f, \quad (27a)$$

$$K_4/K_3 = 0, \quad h \leq h_f. \quad (27b)$$

Clearly, when computing the values of the angle of attack via the feedback control law (26), the glide slope signals are predominant at higher altitudes (approach path), while the absolute path inclination signals are predominant at lower altitudes (flare path). In this way, both the absolute path inclination requirement and the distance requirement can be met.

Results. Numerical results were obtained for the penetration landing guidance scheme, which was implemented in the feedback control form (25)-(26). These results are presented in Fig. 4, which shows the effect of the wind velocity

difference ΔW_x on the guidance trajectory for h_0 = 600 ft. This figure includes two parts: the altitude h versus the distance x; and the velocity V versus the distance x. From the numerical solutions, upon comparing the guidance trajectories (GT), the optimal trajectories (OT), and the nominal trajectory (NT), the following conclusions can be inferred:

(a) for both the GT and the OT, the altitude distribution deviates from that of the NT in the shear region; however, both the GT and OT recover the NT in the aftershear region;

(b) for both the GT and the OT, the deviation from the NT depends on the windshear intensity, increasing as the windshear intensity increases; as expected, the deviation of the GT from the NT is slightly larger than the deviation of the OT from the NT;

(c) for both the GT and the OT, the velocity decreases in the shear region and increases in the aftershear region; the point of minimum velocity occurs at the end of the shear; the minimum velocity of the GT is slightly higher than the minimum velocity of the OT;

(d) for both the GT and the OT, the angle of attack exhibits an initial decrease, followed by a gradual, sustained increase; the peak value of the angle of attack is achieved near the end of the shear; the function $\alpha(t)$ of the OT is smoother than the function $\alpha(t)$ of the GT, which exhibits relatively large oscillations of the angle of attack; these oscillations can be smoothed by employing some more sophisticated form of feedback control than the simple proportional feedback control considered here (see Ref. 12 for details).

4.3. Simplified Guidance. From a practical point of view, it must be emphasized that penetration landing makes sense only if the windshear encounter occurs at lower altitudes; if the windshear encounter occurs at higher altitudes, abort landing must be preferred. Therefore, low-altitude penetration landing deserves particular attention. For this special situation, the guidance scheme of Section 4.2 can be simplified by keeping the power setting at the maximum permissible value and by controlling the angle of attack via only absolute path inclination signals.

Power Setting. For low-altitude penetration landing, the power setting is given by the analytical relations

$$\beta = \beta_0 + \dot{\beta}_0 t, \qquad 0 \leq t \leq \sigma, \quad (28a)$$

$$\beta = 1, \qquad \sigma \leq t \leq \tau. \quad (28b)$$

Here, β is the instantaneous power setting, β_0 is the initial power setting, $\dot{\beta}_0$ is the constant time rate of increase of the power setting, $\sigma = (1 - \beta_0)/\dot{\beta}_0$ is the time at which maximum power setting is reached, and τ is the final time.

Rigorously speaking, Eqs. (28) apply only to the shear portion of the trajectory. However, for low-altitude penetration landing, Eqs. (28) apply also to the aftershear portion of the trajectory, since the time span corresponding to the aftershear portion is small. In the aftershear portion, the power setting must be kept at the maximum value $\beta = 1$, since the velocity at the end of the shear is lower than V_0, and hence a velocity increase is necessary.

Angle of Attack. For low-altitude penetration landing, the guidance law $\gamma_e = \tilde{\gamma}_e(h,F)$ simplifies to $\gamma_e = \tilde{\gamma}_e(h)$. Hence, the feedback control law (26) simplifies to

$$\alpha - \tilde{\alpha}(V) = -K_3[\gamma_e - \tilde{\gamma}_e(h)], \tag{29a}$$

$$K_3 = 5, \tag{29b}$$

$$\alpha \leq \alpha_*, \qquad -\dot{\alpha}_* \leq \dot{\alpha} \leq \dot{\alpha}_*. \tag{29c}$$

Here, α is the instantaneous angle of attack and $\tilde{\alpha}(V)$ is the nominal angle of attack (Ref. 17); γ_e is the instantaneous absolute path inclination and $\tilde{\gamma}_e(h)$ is the nominal absolute path inclination; h is the instantaneous altitude and h_f = 50 ft is the altitude at the end of the approach path/beginning of the flare path; K_3 is the gain coefficient for absolute path inclination error. In turn, the nominal absolute path inclination is given by

$$\tilde{\gamma}_e = \gamma_{e0}, \qquad h \geq h_f, \tag{29d}$$

$$\tilde{\gamma}_e = \gamma_{e0}\, h/h_f + \gamma_{e\tau}(1 - h/h_f), \qquad h \leq h_f. \tag{29e}$$

Comparing the feedback control law (26) and the simplified feedback control law (29), we see that both the glide slope signals and the windshear signals are being ignored. At lower altitudes, ignoring the glide slope signals is permissible in view of Eqs. (27). At lower altitudes, ignoring the windshear signals is also permissible, since the windshear signals are small and priority must be given to achieving the absolute path inclination necessary for safe touchdown.

Results. Numerical results were obtained for the penetration landing simplified guidance scheme, which was implemented in the analytical-feedback control form (28)-(29). These results are presented in Fig. 5, which shows the effect of the wind velocity difference ΔW_x on the simplified guidance trajectories for h_0 = 200 ft. This figure includes two parts: the altitude h versus the distance x; and the velocity V versus the distance x. From the numerical solutions, upon comparing the simplified guidance trajectories (SGT), the optimal trajectories (OT), and the nominal trajectory (NT), the following conclusions can be inferred:

(a) for both the SGT and the OT, the altitude distribution is extremely close to that of the NT and is nearly independent of the wind velocity difference ΔW_x;

(b) for both the SGT and the OT, the point of minimum velocity occurs at the end of the shear; the minimum velocity of the SGT is slightly higher than the minimum velocity of the OT.

5. Conclusions

This paper is concerned with the optimization and guidance of landing trajectories in the presence of windshear. Two aspects of the problem are considered, abort landing and penetration landing. In the former, the only control is the angle of attack, since maximum power setting is employed; in the latter, two controls are involved, the angle of attack and the power setting.

For abort landing, optimal trajectories are determined by minimizing the peak value of the altitude drop. In relatively severe windshears, the optimal trajectory includes three branches: a descending flight branch, followed by a nearly horizontal flight branch, followed by an ascending flight branch, after the aircraft has passed through the shear region. The maximum altitude drop increases with the windshear intensity and the initial altitude. The point of minimum velocity occurs at the end of the shear.

For abort landing, guidance trajectories are developed which are close to the optimal trajectories. The guidance scheme is based on the relative acceleration and is such that the angle of attack is determined by the relative acceleration, the windshear intensity, and the downdraft.

For penetration landing, optimal trajectories are determined by minimizing a performance index measuring the deviation of the altitude of the flight trajectory from that of the nominal trajectory, subject to three requirements: the touchdown path inclination is specified; the touchdown velocity tolerance is specified; and the touchdown distance tolerance is specified. In a relatively severe windshear, the optimal trajectory deviates somewhat from the nominal trajectory in the shear region, but recovers the nominal trajectory in the aftershear region. The deviation increases with the windshear intensity and the initial altitude. The point of minimum velocity occurs at the end of the shear.

For penetration landing, guidance trajectories are developed which are close to the optimal trajectories. The guidance scheme is based on the absolute path inclination, the glide slope angle, and the relative velocity; it is constructed in such a way that the angle of attack is determined by the windshear intensity, the absolute path inclination, and the glide slope angle, while the power setting is determined by the windshear intensity and the relative velocity.

Finally, for low-altitude penetration landing, simplified guidance trajectories are developed which are extremely close to the optimal trajectories. The simplified guidance scheme is based on only the absolute path inclination; it is constructed in such a way that the angle of attack is determined by the absolute path inclination, while the power setting is kept at the maximum permissible value.

References

1. FUJITA, T. T., "The Downburst", Department of Geophysical Sciences, University of Chicago, Chicago, Illinois, 1985.
2. ANONYMOUS, N. N.,"Pan American World Airways, Clipper 759, Boeing 727-235, N4737, New Orleans International Airport, Kenner, Louisiana, July 9, 1982", NTSB Aircraft Accident Report No. 8302, 1983.
3. ANONYMOUS, N. N.,"Delta Air Lines, Lockheed L-1011-3851, N726DA, Dallas-Fort Worth International Airport, Texas, August 2, 1985", NTSB Aircraft Accident Report No. 8605, 1986.
4. FUJITA, T. T., "DFW Microburst", Department of Geophysical Sciences, University of Chicago, Chicago, Illinois, 1986.
5. GORNEY, J. L.,"An Analysis of the Delta 191 Windshear Accident", AIAA Paper No. 87-0626, 1987.
6. ANONYMOUS, N. N., "Flight Path Control in Windshear", Boeing Airliner, pp. 1-12, January-March 1985.
7. ANONYMOUS, N. N., "Windshear Training Aid, Vols. 1 and 2", Federal Aviation Administration, Washington, DC, 1987.
8. MIELE, A., WANG, T., TZENG, C. Y., and MELVIN, W. W., "Optimal Abort Landing Trajectories in the Presence of Windshear", Rice University, Aero-Astronautics Report No. 215, 1987.
9. MIELE, A., WANG, T., TZENG, C. Y., and MELVIN, W. W.,"Abort Landing Guidance Trajectories in the Presence of Windshear", Rice University, Aero-Astronautics Report No. 217, 1987.

10. MIELE, A., WANG, T., and MELVIN, W. W., "Acceleration, Gamma, and Theta Guidance Schemes for Abort Landing Trajectories in the Presence of Windshear", Rice University, Aero-Astronautics Report No. 223, 1987.

11. MIELE, A., WANG, T., WANG, H., and MELVIN, W. W., "Optimal Penetration Landing Trajectories in the Presence of Windshear", Rice University, Aero-Astronautics Report No. 216, 1987.

12. MIELE, A., WANG, T., and MELVIN, W. W., "Penetration Landing Guidance Trajectories in the Presence of Windshear", Rice University, Aero-Astronautics Report No. 218, 1987.

13. PSIAKI, M. L., and STENGEL, R. F.,"Optimal Flight Paths through Microburst Wind Profiles", Journal of Aircraft, Vol. 23, pp. 629-635, 1986.

14. CHU, P. G., and BRYSON, A. E., Jr.,"Control of Aircraft Landing Approach in Windshear", AIAA Paper No. 87-0632, 1987.

15. MIELE, A., and WANG, T.,"Primal-Dual Properties of Sequential Gradient-Restoration Algorithms for Optimal Control Problems, Part 1,Basic Problem", Integral Methods in Science and Engineering, Edited by F. R. Payne et al, Hemisphere Publishing Corporation, Washington, DC, pp. 577-607, 1986.

16. MIELE, A., and WANG, T., "Primal-Dual Properties of Sequential Gradient-Restoration Algorithms for Optimal Control Problems, Part 2, General Problem",Journal of Mathematical Analysis and Applications, Vol. 119, pp. 21-54, 1986.

17. MIELE, A., WANG, T., and MELVIN, W. W., "Optimization and Acceleration Guidance of Flight Trajectories in a Windshear", Journal of Guidance, Control, and Dynamics, Vol. 10, pp. 368-377, 1987.

18. IVAN, M.,"Ring-Vortex Downburst Model for Flight Simulation",Journal of Aircraft, Vol. 23, pp. 232-236, 1986.

List of Captions

Fig. 1. Wind functions A(x) and B(x).

Fig. 2A. Abort landing, optimal trajectories (OT) and guidance trajectories (GT): altitude h versus time t (ΔW_x = 120 ft sec^{-1}).

Fig. 2B. Abort landing, optimal trajectories (OT) and guidance trajectories (GT): velocity V versus time t (ΔW_x = 120 ft sec^{-1}).

Fig. 3A. Abort landing, optimal trajectories (OT) and guidance trajectories (GT): altitude h versus time t (h_0 = 600 ft).

FIg. 3B. Abort landing, optimal trajectories (OT) and guidance trajectories (GT): velocity V versus time t (h_0 = 600 ft).

Fig. 4A. Penetration landing, optimal trajectories (OT) and guidance trajectories (GT): altitude h versus distance x(h_0 = 600 ft).

Fig. 4B. Penetration landing, optimal trajectories (OT) and guidance trajectories (GT): velocity V versus distance x (h_0 = 600 ft).

Fig. 5A. Penetration landing, optimal trajectories (OT) and simplified guidance trajectories (SGT): altitude h versus distance x (h_0 = 200 ft).

Fig. 5B. Penetration landing, optimal trajectories (OT) and simplified guidance trajectories (SGT): velocity V versus distance x (h_0 = 200 ft).

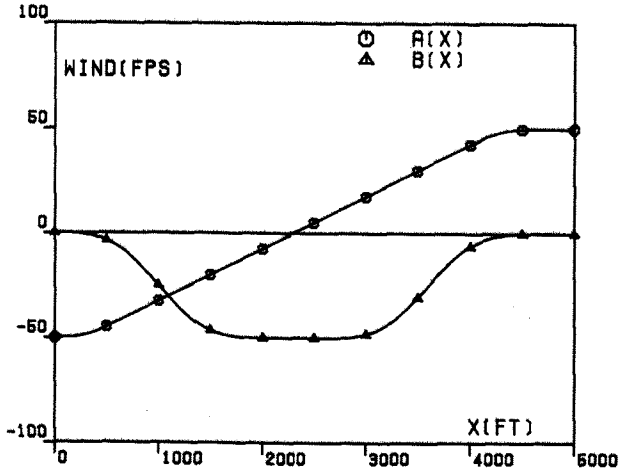

FIG. 1. WIND FUNCTIONS.

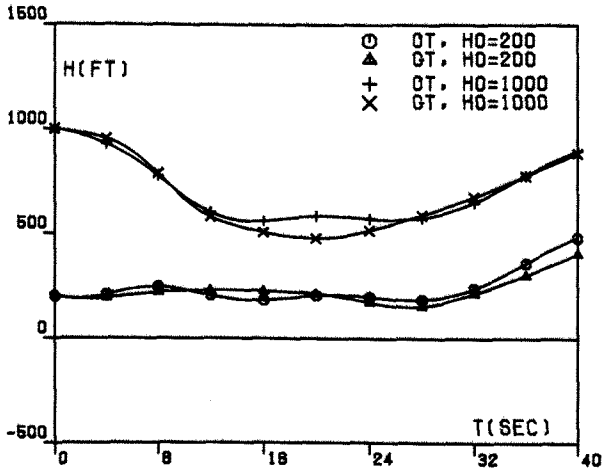

FIG. 2A. ABORT LANDING TRAJECTORIES, DWX=120FPS.

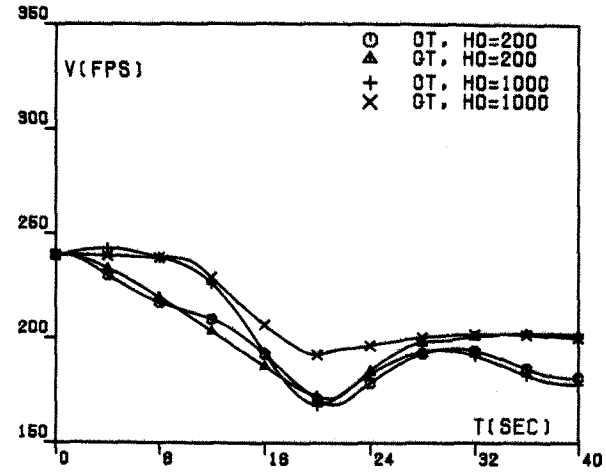

FIG. 2B. ABORT LANDING TRAJECTORIES, DWX=120FPS.

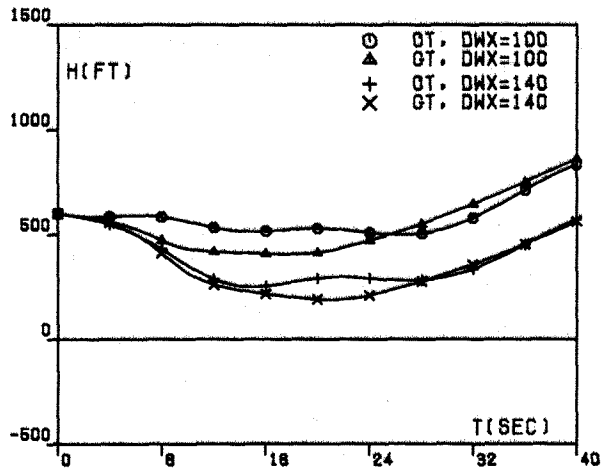

FIG. 3A. ABORT LANDING TRAJECTORIES, HO=600FT.

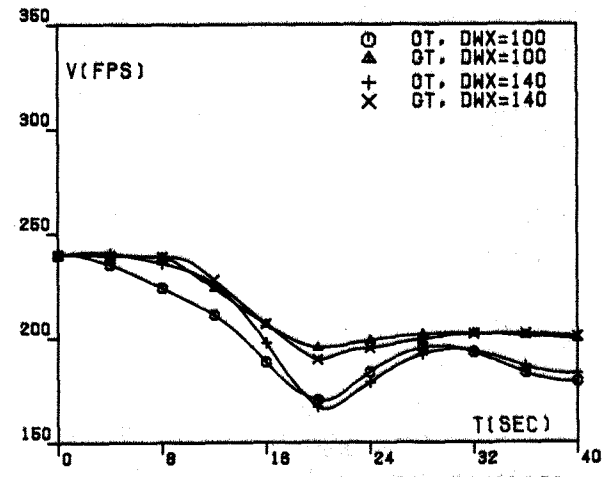

FIG. 3B. ABORT LANDING TRAJECTORIES, HO=600FT.

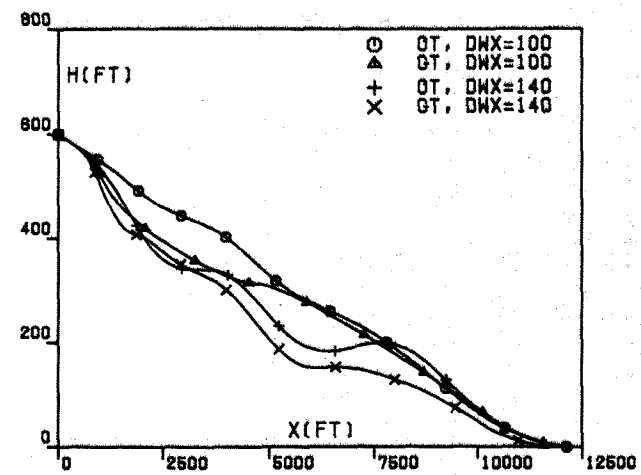

FIG. 4A. PENETRATION LANDING TRAJECTORIES, HO=600FT.

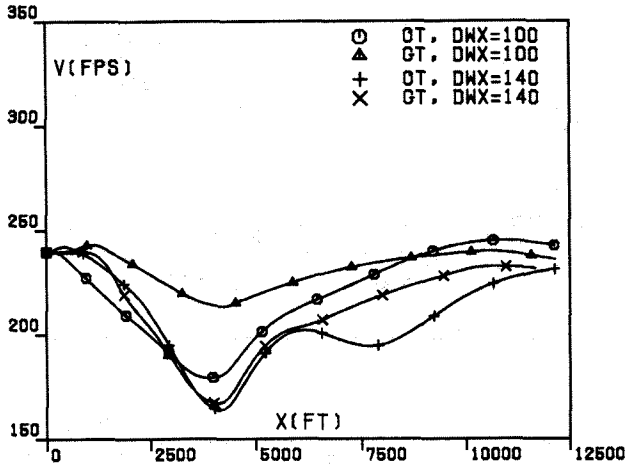

FIG. 4B. PENETRATION LANDING TRAJECTORIES, HO=600FT.

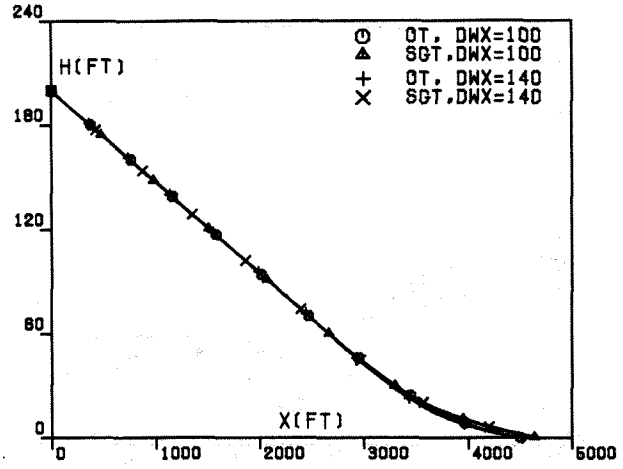

FIG. 5A. PENETRATION LANDING TRAJECTORIES, HO=200FT.

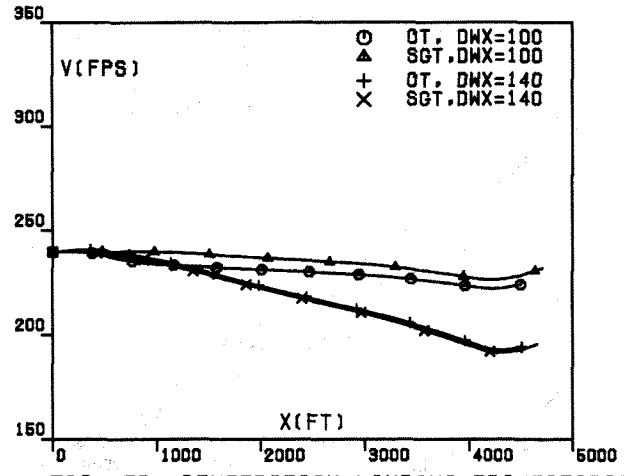

FIG. 5B. PENETRATION LANDING TRAJECTORIES, HO=200FT.